AIP Applied Physics Letters

Superconducting a-WxSi1x nanowire single-photon detector with saturated internal quantum efficiency from visible to 1850 nm

Burm Baek, Adriana E. Lita, Varun Verma, and Sae Woo Nam

Citation: Appl. Phys. Lett. **98**, 251105 (2011); doi: 10.1063/1.3600793

View online: http://dx.doi.org/10.1063/1.3600793

View Table of Contents: http://apl.aip.org/resource/1/APPLAB/v98/i25

Published by the American Institute of Physics.

Related Articles

Pound-locking for characterization of superconducting microresonators
Rev. Sci. Instrum. 82, 104706 (2011)

Thin-film superconducting resonator tunable to the ground-state hyperfine splitting of 87Rb
AIP Advances 1, 042107 (2011)

Surface loss simulations of superconducting coplanar waveguide resonators
Appl. Phys. Lett. 99, 113513 (2011)

Modelling the resistive state in a transition edge sensor
Appl. Phys. Lett. 99, 063503 (2011)

Little–Parks oscillations at low temperatures: Gigahertz resonator method
Appl. Phys. Lett. 98, 242504 (2011)

Additional information on Appl. Phys. Lett.

Journal Homepage: http://apl.aip.org/

Journal Information: http://apl.aip.org/about/about_the_journal

Top downloads: http://apl.aip.org/features/most_downloaded

Information for Authors: http://apl.aip.org/authors

ADVERTISEMENT

Downloaded 28 Oct 2011 to 132.163.53.60. Redistribution subject to AIP license or copyright; see http://apl.aip.org/about/rights_and_permissions

Superconducting a-W_xSi_{1-x} nanowire single-photon detector with saturated internal quantum efficiency from visible to 1850 nm

Burm Baek,[a] Adriana E. Lita, Varun Verma, and Sae Woo Nam
National Institute of Standards and Technology, 325 Broadway, Boulder, Colorado 80305, USA

(Received 6 May 2011; accepted 27 May 2011; published online 21 June 2011)

We have developed a single-photon detector based on superconducting amorphous tungsten–silicon alloy (a-W_xSi_{1-x}) nanowire. Our device made from a uniform a-W_xSi_{1-x} nanowire covers a practical detection area ($16\ \mu m \times 16\ \mu m$) and shows high sensitivity featuring a plateau of the internal quantum efficiencies, i.e., efficiencies of generating an electrical pulse per absorbed photon, over a broad wavelength and bias range. This material system for superconducting nanowire detector technology could overcome the limitations of the prevalent nanowire devices based on NbN and lead to more practical, ideal single-photon detectors having high efficiency, low noise, and high count rates. © *2011 American Institute of Physics*. [doi:10.1063/1.3600793]

Superconducting nanowire single-photon detectors (SNSPDs) based on NbN (Refs. 1 and 2) have played a crucial role in significant high-fidelity quantum optics measurements.[3–5] They are sensitive over a broad range of wavelengths, with a low dark count rate and high timing resolution that are unmatched by other single-photon detector technologies. However, the low quantum efficiency has been the limiting factor in many correlation-type measurements such as photon statistics,[6] quantum state tomography,[4] and quantum key distribution.[3] For these measurements, the integration period decreases rapidly as η^n, where n is the order of the correlation and η is the quantum efficiency. In some quantum optical measurements, extremely high detection efficiency is even a fundamental requirement; linear optical quantum computing[7] and loophole-free Bell tests[8] are the most prominent examples requiring such high efficiency detectors.

The difficulty in achieving SNSPDs of high efficiency stems from their unique internal mechanism of photon detection and the resultant extreme geometry.[1,2,9,10] An absorbed photon in a superconducting nanowire results in a large number of broken Cooper pairs that carry the bias current in the superconducting state. If the bias current is less than, but close to, the superconducting critical current I_c, a resistive cross-section can be created after absorbing the photon that can be observed. Since this detection process requires a very small geometric cross-section, an SNSPD is typically made as a narrow nanowire ($\sim$100 nm wide) from a very thin film ($\sim$4 nm thick). A reasonable efficiency is reached only when the device is operated with a bias current very close to I_c. Constrictions in the nanowire limit the critical current, which subsequently reduces the sensitivity of the nanowire to incident photons.[11] Consequently, very high material and fabrication uniformity is required to make the entire nanowire sensitive. Recently, wire widths of 20–50 nm in a parallel nanowire scheme have been fabricated to enhance sensitivity to mid-infrared photons.[12,13] However, fabricating these devices over a large area suitable for near-unity light coupling, remains challenging.

In this letter, we show our development of a nanowire device based on an a-W_xSi_{1-x} thin film that overcomes the limitations of devices based on the conventional nitride superconductors (NbN and NbTiN). a-W_xSi_{1-x} has a tunable superconducting transition temperature T_c up to 5 K that depends on the stoichiometry.[14] We expect larger hot spots in an a-W_xSi_{1-x} nanowire than those in NbN for the following reasons. The superconducting gap energy is smaller, and thus more Cooper pairs are broken when a photon is absorbed.[9] Also, the low electron density, inferred from the low critical current density, could contribute to the creation of larger hot spots.[9] Extreme structural homogeneity and the absence of grain boundaries in an amorphous film could be advantageous compared with the granular structure in nitride superconductors,[15] despite potential compositional nonuniformity. By addressing both the energy sensitivity and the structural homogeneity, we expect higher internal quantum efficiency in an a-W_xSi_{1-x} detector with a geometry similar to those of conventional SNSPDs.

In our samples, the a-W_xSi_{1-x} thin film is grown with a nominal Si content $\sim$25% on an oxidized 3″ Si wafer by cosputtering W and Si. We obtained an amorphous structure as verified by x-ray diffraction, and we measured the maximized T_c of 5 K in $\sim$60-nm-thick film. A 4.5-nm-thick film was used for the device fabrication. The nanowires were defined by electron beam lithography with 50-nm-thick poly-(methyl methacrylate) as resist, followed by reactive ion etching in SF_6 [Fig. 1(a)]. The fabricated nanowire has T_c $\sim$3 K due to the reduced thickness[16] [Fig. 1(b)] and the processing steps required for the meander patterning. We patterned the film into a nanowire with a width of 150 nm and a pitch of 250 nm, resulting in a filling fraction of 0.6.

We made devices as large as $16\ \mu m \times 16\ \mu m$ so that we could optically couple the device by butt-coupling to a standard telecommunications single-mode fiber core of $\sim$10 μm diameter. We used a compact mechanical packaging scheme described in a previous work.[17] The packaged device is mounted on the lowest-temperature stage of a cryogen-free adiabatic demagnetization refrigerator capable of cooling our device below 0.1 K.

The maximum applicable bias current for a normal operation of the device increases as the temperature decreases and is nearly constant at $\sim$5.4 μA for temperatures below

[a]Electronic mail: burm.baek@nist.gov.

 © 2011 American Institute of Physics

Downloaded 28 Oct 2011 to 132.163.53.60. Redistribution subject to AIP license or copyright; see http://apl.aip.org/about/rights_and_permissions

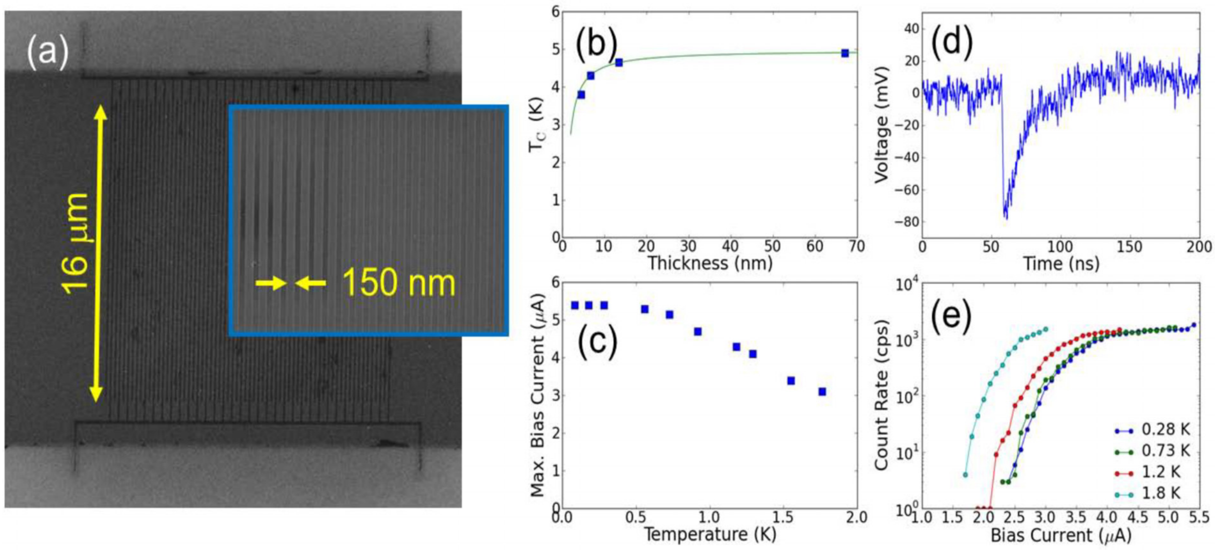

FIG. 1. (Color online) Superconducting a-W_xSi_{1-x} nanowire single-photon detector. (a) Scanning electron micrograph of a 16 μm×16 μm a-W_xSi_{1-x} meander area. Inset: a zoomed image showing well-defined 150-nm-wide nanowires. (b) Measured superconducting transition temperature vs a-W_xSi_{1-x} film thickness (square) and a fit (line). (c) Measured maximum bias current for a normal operation of the device vs temperature in an a-W_xSi_{1-x} device. (d) A single-shot oscilloscope trace of an amplified electrical pulse of an a-W_xSi_{1-x} device. The device was illuminated by an attenuated 1550 nm cw laser. The amplifier gain and bandwidth are 52 dB and 500 MHz. (e) Count rate of background light leakage vs bias current with the fiber port blocked from light.

0.5 K [Fig. 1(c)]. At $T<2$ K, we can detect electrical pulses induced by photon detection from the device with a proper bias current and illumination. The pulses are significantly larger than the amplifier noise level [Fig. 1(d)], with a (1/e) rise time of ~2 ns, limited by our amplifier bandwidth, and a (1/e) recovery period of ~14 ns, limited by the kinetic inductance of the device. We did not explore the latching behavior of the device because the device described in this letter reaches the maximum efficiency at a relatively low bias current as shown in the next paragraph. We observed a slowly increasing background count rate when increasing bias current up to ~1.5 kcps for the fiber-coupled device, with the room light turned off and the fiber port covered [Fig. 1(e)]. However, we detected no counts when the device was not fiber coupled; the dark count rate was <1 Hz at a bias up to 98% of the maximum bias current with the integration time >10 s. This indicates all the background counts either come from stray light or from blackbody radiation coupled into the fiber, instead of from the thermal fluctuation in the device itself over the measurement bias range.

We carried out photon counting measurements with a fiber-coupled 1550 nm continuous-wave (cw) diode laser with the polarization optimized for the maximum detection efficiency. The photon flux was calculated by use of a calibrated optical power meter and calibrated attenuators.[18] We varied the optical intensity, keeping it at a low level to make sure the count rate changes linearly with the intensity. Our measurements represent the total detector system efficiency and include no corrections to compensate for the losses in the fiber, the coupling of the input fiber connector to the detector system, or the fiber-coupled detector package. The device efficiency as a function of bias was nearly constant below 0.5 K, which is consistent with the temperature dependence of the maximum bias current. We measured ~20% detector system efficiency [Fig. 2(a)] which is the highest efficiency we have observed so far by use of our compact detector packages with front-side fiber coupling. The efficiency stays remarkably constant over a wide range of bias, in contrast to the conventional nitride devices. This saturation behavior is also observed at higher temperatures, up to 1.6 K. We interpret this as the device reaching the limit of the internal quantum efficiency. The high internal sensitivity over a wide range of bias current shown here should relax the usual stringent requirement of highly uniform I_c distribution over the entire length of the nanowire for a device with a practical area.

The wavelength dependence of efficiency is an important measure of detector performance, and also provides in-

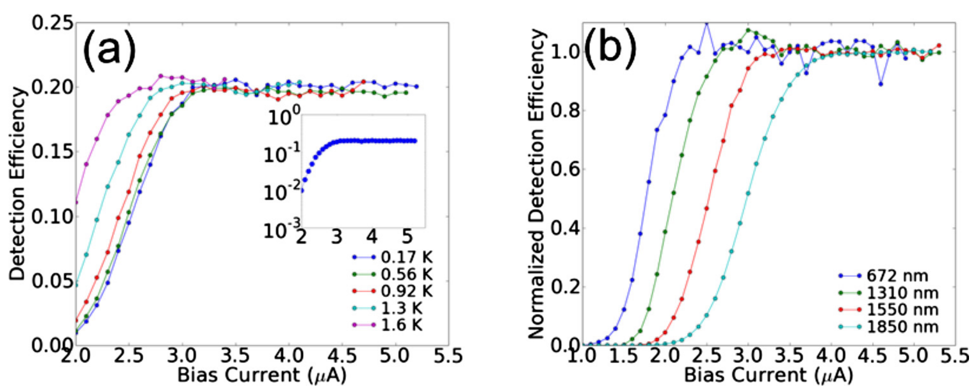

FIG. 2. (Color online) Bias dependence of the detector system efficiency. (a) Detector system efficiency vs bias current at different temperatures. The device was illuminated by an attenuated 1550 nm cw laser. Inset: the efficiency plot at 0.17 K on a semi-log scale. (b) Normalized detection efficiency vs bias current with different wavelengths.

Downloaded 28 Oct 2011 to 132.163.53.60. Redistribution subject to AIP license or copyright; see http://apl.aip.org/about/rights_and_permissions

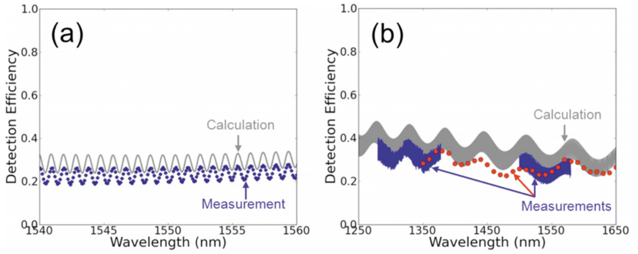

FIG. 3. (Color online) Wavelength dependence of the detector system efficiency. Measured efficiencies and calculated spectral absorptances are plotted together for comparison. (a) Plot in a narrow wavelength range around 1550 nm, showing the fine interference pattern. (b) Plot of detection efficiency over a wide wavelength range. Measurement results using coarse wavelength steps from a white light source (circles) are plotted together with data from two tunable lasers (1550 and 1310 bands). The fine interference patterns shown in (a) cannot be clearly resolved in this plot and appear as bands.

formation on the device structure and physics. We used laser diodes tunable around 1310 nm and 1550 nm and a white light source[19] for fine and coarse wavelength scanning, respectively. We observed a broad plateau in efficiency with different wavelengths in a range of 672–1850 nm [Fig. 2(b)]. For longer wavelengths, the saturation range becomes narrower and the transition range becomes wider. This saturated sensitivity occurs even for a long wavelength of 1850 nm, indicating the potential for high broadband sensitivity from visible to near-infrared and potentially to mid-infrared. As shown in Fig. 3, the efficiency as a function of wavelength is significantly affected by the optical interferences due to the presence of partially reflecting surfaces in the optical path in the device and the fiber-coupled package. The oscillations in Fig. 3(a), shown over the telecommunications band near 1550 nm, are due to the reflections from the top and bottom surfaces of the detector chip. The larger scale modulation shown in Fig. 3(b) is due to the interference of the reflections from the fiber tip and the detector surface; these allow us to extract the fiber-to-detector gap of $\sim 17\ \mu$m. The coarse step measurement using a white light source provides a reasonable estimation of the efficiencies in the wavelength range not covered by the lasers [Fig. 3(b)]. Other than such structural features, the efficiency is maintained high between 19% and 40% without significant roll-off in a wavelength range of 1280–1650 nm. This is a remarkable improvement in comparison with the conventional nitride devices that typically show exponentially decreasing efficiencies with increasing wavelength.[10,19]

We estimated the optical absorption using the optical constants of a-W_xSi_{1-x} extracted from spectrophotometry measurements of unpatterned thin film samples at room temperature and the effective medium approximation for a nanowire grid structure.[19] The estimated absorption reproduces the trend of the efficiency measurement results, including the interference patterns, and shows that the detection efficiencies are close to the optical absorption (Fig. 3). The deficit is approximately 0.9 dB over the measurement wavelength range; this implies an internal quantum efficiency of at least $\sim$80%. The internal quantum efficiency could be higher because of loss in the fiber link in our detector system and the accuracy of the estimated optical absorption. Better estimation of the internal efficiency is beyond the scope of this letter but may be achieved by direct optical measurements on the device *in situ*.[19,20]

In summary, we have demonstrated an SNSPD that utilizes a-W_xSi_{1-x} as the absorbing medium. Our device has demonstrated a detector system efficiency of 19%–40% over a wavelength range of 1280–1650 nm. This is a significant improvement compared with the conventional, fiber-coupled NbN SNSPDs with an efficiency $<10\%$.[17,19] We have also demonstrated that our device have a plateau in internal quantum efficiency with large nanowire widths compared with those of conventional SNSPDs. This is a significant accomplishment, as it relaxes the fabrication tolerances, enabling higher yields and larger area detectors. A detector system with efficiency $>80\%$ could be achieved with a high yield by implementing the integrated optical cavity technology[21,22] in the near future.

This work was supported by the NIST Quantum Information initiative. We acknowledge Justin Shaw for assistance with x-ray diffraction measurements for our a-W_xSi_{1-x} films and Richard Mirin for the comments on the manuscript.

[1] G. N. Gol'tsman, O. Okunev, G. Chulkova, A. Lipatov, A. Semenov, K. Smirnov, B. Voronov, and A. Dzardanov, Appl. Phys. Lett. **79**, 705 (2001).
[2] R. H. Hadfield, Nat. Photonics **3**, 696 (2009).
[3] H. Takesue, S. W. Nam, Q. Zhang, R. H. Hadfield, T. Honjo, K. Tamaki, and Y. Yamamoto, Nat. Photonics **1**, 343 (2007).
[4] J. Chen, J. B. Altepeter, M. Medic, K. F. Lee, B. Gokden, R. H. Hadfield, S. W. Nam, and P. Kumar, Phys. Rev. Lett. **100**, 133603 (2008).
[5] C. Clausen, I. Usmani, F. Bussie′res, N. Sangouard, M. Afzelius, H. de Ridematten, and N. Gisin, Nature (London) **469**, 508 (2011).
[6] M. J. Stevens, B. Baek, E. A. Dauler, A. J. Kerman, R. J. Molnar, S. A. Hamilton, K. K. Berggren, R. P. Mirin, and S. W. Nam, Opt. Express **18**, 1430 (2010).
[7] E. Knill, R. Laflamme, and G. J. Milburn, Nature (London) **409**, 46 (2001).
[8] A. Cabello, A. Rossi, G. Vallone, F. De Martini, and P. Mataloni, Phys. Rev. Lett. **102**, 040401 (2009).
[9] A. D. Semenov, G. N. Gol'tsman, and A. A. Korneev, Physica C **351**, 349 (2001).
[10] A. Verevkin, J. Zhang, R. Sobolewski, A. Lipatov, O. Okunev, G. Chulkova, A. Korneev, K. Smirnov, and G. N. Gol'tsman, Appl. Phys. Lett. **80**, 4687 (2002).
[11] A. J. Kerman, E. A. Dauler, J. K. W. Yang, K. M. Rosfjord, V. Anant, K. Berggren, G. N. Gol'tsman, and B. M. Voronov, Appl. Phys. Lett. **90**, 101110 (2007).
[12] Y. Korneeva, I. Florya, A. Semenov, A. Korneev, and G. Goltsman, IEEE Trans. Appl. Supercond. **21**, 323 (2011).
[13] F. Marsili, F. Najafi, E. Dauler, F. Bellei, X. Hu, M. Csete, R. J. Molnar, and K. K. Berggren, Nano Lett **11**, 2048 (2011).
[14] S. Kondo, J. Mater. Res. **7**, 853 (1992).
[15] S. Wolf and W. H. Lowrey, Phys. Rev. Lett. **39**, 1038 (1977).
[16] D. B. Haviland, Y. Liu, and A. M. Goldman, Phys. Rev. Lett. **62**, 2180 (1989).
[17] R. H. Hadfield, M. J. Stevens, S. S. Gruber, A. J. Miller, R. E. Schwall, R. P. Mirin, and S. W. Nam, Opt. Express **13**, 10846 (2005).
[18] A. E. Lita, A. J. Miller, and S. W. Nam, Opt. Express **16**, 3032 (2008).
[19] B. Baek, J. A. Stern, and S. W. Nam, Appl. Phys. Lett. **95**, 191110 (2009).
[20] V. Anant, A. J. Kerman, E. A. Dauler, J. K. W. Yang, K. M. Rosfjord, and K. K. Berggren, Opt. Express **16**, 10750 (2008).
[21] D. Rosenberg, S. W. Nam, A. J. Miller, A. Salminen, E. Grossman, R. E. Schwall, and J. M. Martinis, Nucl. Instrum. Methods Phys. Res. A **520**, 537 (2004).
[22] K. M. Rosfjord, J. K. W. Yang, E. A. Dauler, A. J. Kerman, V. Anant, B. M. Voronov, G. N. Gol'tsman, and K. K. Berggren, Opt. Express **14**, 527 (2006).

Downloaded 28 Oct 2011 to 132.163.53.60. Redistribution subject to AIP license or copyright; see http://apl.aip.org/about/rights_and_permissions